Heliyon 10 (2024) e38701

Contents lists available at ScienceDirect

Heliyon

journal homepage: www.cell.com/heliyon

Research article

Effects of Shaofu Zhuyu decoction on intestinal flora and fibrosis in a mouse model of endometriosis

Bing-Bing Li [a], Qing-Qing Xun [b], Chao Wei [a], Bin Yu [a], Xue Pan [c,**], Qian Shen [d,*]

[a] College of Integrated Chinese and Western Medicine, Jining Medical University, Jining, 272000, Shandong Province, China
[b] School of Clinical Medicine, Jining Medical University, Jining, 272000, Shandong Province, China
[c] Third Affiliated Hospital, Beijing University of Chinese Medicine, Beijing, 100029, China
[d] Guang'anmen Hospital, China Academy of Chinese Medical Sciences, Beijing, 100053, China

ARTICLE INFO

Keywords:
Shaofu Zhuyu decoction
Endometriosis
Intestinal flora
Fibrosis
Metabolism

ABSTRACT

Shaofu Zhuyu decoction has been widely used to treat gynecological diseases; however, its mechanism of action in endometriosis remains unclear. We analyzed Shaofu Zhuyu decoction's chemical composition using ultra-high performance liquid chromatography-mass spectrometry. In an endometriosis mouse model, ectopic lesions weight measurements and hematoxylin and eosin staining were used to assess the therapeutic efficacy of Shaofu Zhuyu decoction. Effects on intestinal microflora were analyzed using 16S ribosomal ribonucleic acid sequencing, and impacts on focal fibrosis were analyzed using Masson's trichrome staining. Moreover, fibrosis- and metabolism-related proteins were assessed using immunohistochemistry and enzyme-linked immunosorbent assay. The study identified 157 chemical constituents within Shaofu Zhuyu decoction. Shaofu Zhuyu decoction treatment in mice with endometriosis resulted in a reduction in ectopic lesions weight ($P < 0.05$) and delayed disease progression. Moreover, it improved the diversity and abundance of intestinal flora, and decreased the expression of Lachnospiraceae ($P < 0.05$), Rikenellaceae ($P < 0.01$), Ruminococcaceae ($P < 0.01$), Lachnoclostridium ($P < 0.05$), and unclassified_f_Ruminococcaceae ($P < 0.05$). Kyoto Encyclopedia of Genes and Genomes analysis revealed enrichment in carbohydrate, amino acid, and lipid metabolism pathways. Masson's trichrome staining revealed that compared to the untreated group, the Shaofu Zhuyu decoction group exhibited significantly reduced collagen deposition areas ($P < 0.001$), lower TGF-β1 ($P < 0.001$), COL1A1 ($P < 0.05$), and α-SMA ($P < 0.01$) expression in ectopic lesions, along with increased serum adiponectin ($P < 0.05$), decreased serum TGF-β1 ($P < 0.001$), and CTGF ($P < 0.05$). Shaofu Zhuyu decoction regulates the intestinal flora of mice with endometriosis while also reducing fibrosis at the lesion site. These findings highlight novel mechanisms for its efficacy in alleviating endometriosis.

1. Introduction

Endometriosis predominantly occurs in women of childbearing age, with an incidence of approximately 6%–10 %. As a chronic neuroinflammatory and hormone-dependent gynecological disease, it mainly manifests as dysmenorrhea, chronic pelvic pain, and

* Corresponding author. No.5 North Line Pavilion, Xicheng District, Beijing, China.
** Corresponding author. 51 Xiaoguan Street, Anwai, Chaoyang District, Beijing, China.
E-mail addresses: panx1346@126.com (X. Pan), sh-qian@qq.com (Q. Shen).

https://doi.org/10.1016/j.heliyon.2024.e38701
Received 6 January 2024; Received in revised form 1 September 2024; Accepted 27 September 2024
Available online 1 October 2024

infertility [1]. At present, endometriosis is mainly treated via surgical resection of ectopic lesions or through the administration of non-steroidal anti-inflammatory or hormonally active drugs; however, these pharmacological agents often fail to effectively improve the symptoms women with the disease experience. In addition, more than 50 % of patients require further surgical intervention within 5 years, and these individuals are more susceptible to the development of ovarian cancer [2]. Therefore, there is an urgent need for more effective clinical treatments for patients with endometriosis. Shaofu Zhuyu decoction (SFZYD), which is used in traditional Chinese medicine, could be an effective treatment option.

SFZYD was derived from the *Correction of the Errors of Medical Works*, which was written by Wang Qingren during the Qing Dynasty. SFZYD is composed of 10 herbs and can promote blood circulation, alleviate blood stasis, warm meridians, and relieve pain. These effects have led to SFZYD being widely used for the clinical management of various gynecological diseases, although the mechanisms are unclear.

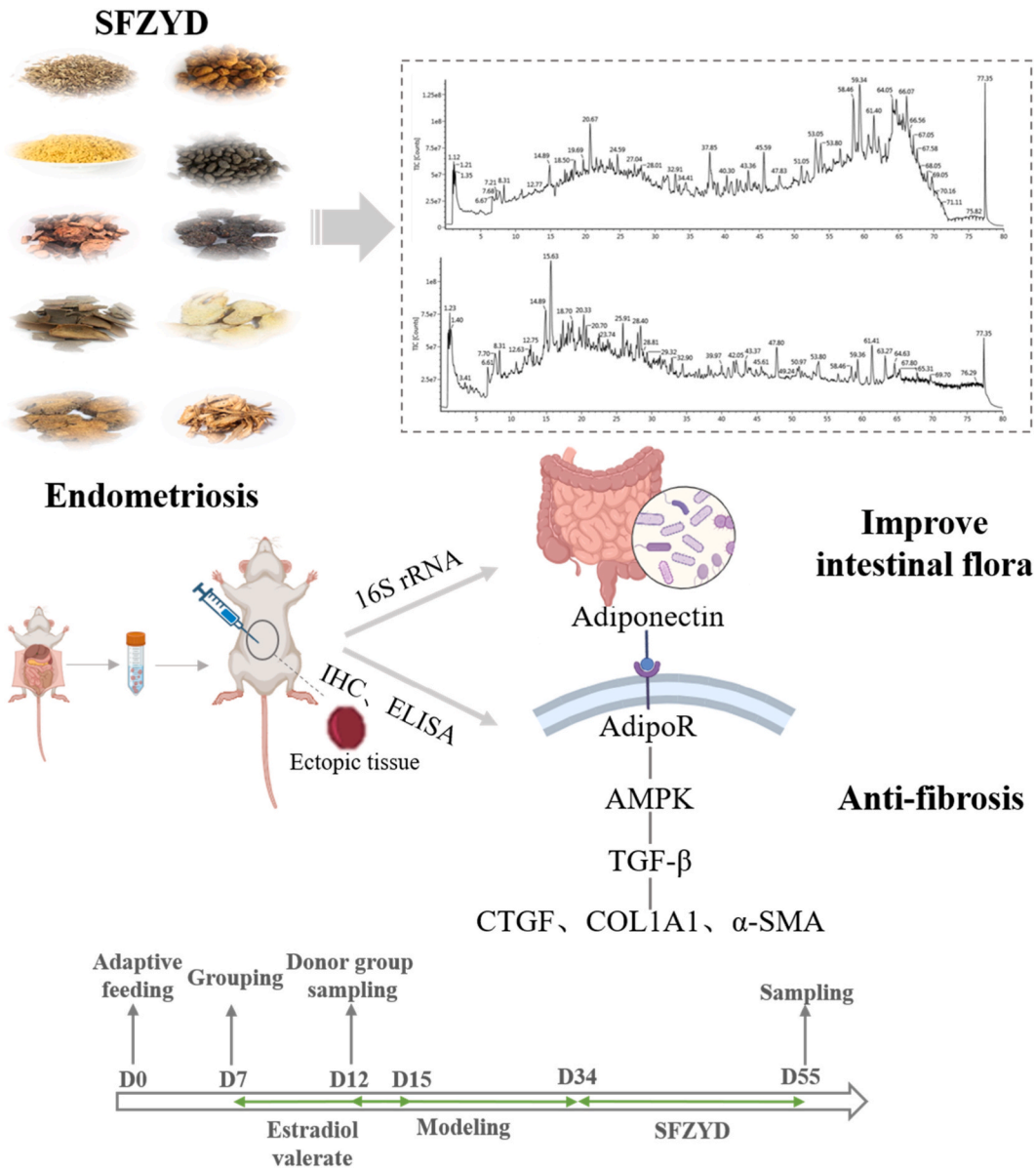

Fig. 1. Graphic summary. The top panels depict the analysis of the key constituents of SFZYD using UPLC-MS/MS. The lower panels depict the generation of the mouse model of endometriosis and quantification of changes in expression in ectopic tissues using 16S rRNA, IHC, and ELISA, which revealed improvements in the intestinal flora and enhancement of anti-fibrotic signaling. SFZYD: Shaofu Zhuyu decoction; UPLC-MS/MS: ultra-high performance liquid chromatography-mass spectrometry/mass spectrometry; rRNA: ribosomal ribonucleic acid; IHC: immunohistochemistry; ELISA: enzyme-linked immunosorbent assay; AdipoR: adiponectin receptor; AMPK: adenosine monophosphate-activated protein kinase; TGF-β: transforming growth factor beta; CTGF: connective tissue growth factor; COL1A1: collagen type I alpha 1; α-SMA: alpha-smooth muscle actin.

Intestinal microbes form a complex microbial community of bacteria, fungi, and viruses that not only play an important role in intestinal physiology and pathology, but they can also act as a kind of endocrine organ, influencing the function of parenteral organs through various biological pathways. Increasing evidence has shown that homeostatic imbalances in the intestinal microbiome can lead to the development of various diseases, and there is clear evidence of a link between intestinal microbes and the development of endometriosis [3], mainly through the regulation of estrogen levels, immunity, and inflammatory pathways [4]. For example, Chadchan et al. demonstrated that the intestinal microbiome is necessary for the development of endometriosis in mice, affecting its progression by regulating the peritoneal immune cell population, and the quinic acid produced by intestinal microbes can promote the growth of ectopic endometrial tissue [5]. Those researchers have also shown that gut-derived n-butyrate protects against endometriosis by activating the expression of Rap1 guanosine triphosphatase activating protein and by inhibiting the Rap1 oncogenic pathway [6]. *Escherichia coli* has been shown to be abundant in the intestinal tract of patients with endometriosis and can affect the development of the disease by stimulating β-glucuronidase expression and increasing the concentration of circulating estrogen [7]. Additionally, some probiotics, including *Lactobacillus gasseri*, have been used to alleviate symptoms in patients with endometriosis [8].

Given the link between the intestinal microbiome and endometriosis and the ability of SFZYD to alleviate symptoms of gynecological diseases, the aim of this study was to investigate the effects and potential mechanisms of SFZYD in a mouse model of endometriosis, which involved allograft transplantation, using 16S ribosomal ribonucleic acid (rRNA) sequencing and other techniques (Fig. 1).

2. Materials and methods

2.1. Animals

Twenty-four 8-week-old female BALB/c mice were purchased from Jinan Pengyue Experimental Animal Breeding Co., Ltd. (Animal Qualification Certificate: SCXK(Lu)20220006). All mice were maintained under standard conditions (12 h/12 h light/dark cycle at 22–24 °C and 50 % relative humidity) and provided unrestricted access to food and water. After a one-week acclimatization period, the mice were randomly assigned to one of the following four groups at the beginning of the experiment: control group (n = 6), donor group (n = 6), model group (n = 6), and SFZYD treatment group (n = 6). Drug administration via intragastric gavage was conducted while the mice were conscious; however, discomfort was minimized by using straight gavage needles that were appropriate for the 15–17-g body weight of the animals (22-gauge, 1-inch length, and 1.25-mm ball diameter). All animals were euthanized by barbiturate overdose (intraperitoneal injection, 30 mg/kg pentobarbital sodium) for tissue collection. All animal experiments were approved by the Animal Experiment Ethics Subcommittee of Jining Medical University (No. JNMC-2023-DW-150).

2.2. Establishment of the endometriosis model

Mouse models of endometriosis have been previously established via intraperitoneal injection of uterine fragments [9,10]. In the present study, estradiol valerate (0.5 mg/kg) was administered by gavage to donor and recipient mice for five consecutive days to, and the donor mice were subsequently anesthetized. After opening the abdominal cavity, the uterus was quickly removed and transferred into pre-cooled normal saline to eliminate the blood and mucus. The uterus was divided into two parts, and each half was placed into a Petri dish containing 0.5 mL of normal saline. The uterus was cut lengthwise with ophthalmic scissors to expose the endometrial surface, then cut into small 1-mm^2 pieces. Each bisected uterus of a donor mouse was injected into the disinfected abdomens of two recipient mice (one mouse from the model group and one mouse from the SFZYD group). After establishment of the model, estradiol valerate (0.5 mg/kg) was continuously injected into the stomach of the mice for 3 days to promote the growth of ectopic lesions. The stability of the model was confirmed three weeks after surgery.

2.3. Drug administration

SFZYD was uniformly prepared in pellet form by Jiangyin Tianjiang Pharmaceutical Co., Ltd. SFZYD includes 10 kinds of Chinese herbs (Table 1). The pellet was dissolved in saline and stored at 4 °C until further use. The required dose of SFZYD was calculated

Table 1
The traditional Chinese medicine composition of SFZYD.

Chinese name	Latin name	Weight (g)
Dang gui	*Angelicae Sinensis Radix*	9
Chi shao	*Radix Paeoniae Rubra*	6
Yan hu suo	Corydalis Rhizoma	3
Mo yao	*Myrrha*	6
Chuan xiong	*Chuanxiong Rhizome*	9
Wu ling zhi	*Trogopterus Dung*	6
Pu huang	*Pollen Typhae*	9
Gan jiang	*Zingiberis Rhizome*	3
Xiao hui xiang	*Foeniculi Fructus*	3
Rou gui	*Cinnanmomi Cortex*	3

according to the equivalent dose formula for humans and animals described in the third edition of Experimental Methodology in Pharmacology [11]. Mice in the treatment group were administered SFZYD at a dose of 8.645 g/kg via oral gavage once daily for 21 days, whereas the mice in the control and model groups received an equivalent volume of normal saline by oral gavage.

2.4. Chemical analysis of SFZYD by mass spectrometry (MS)

Liquid chromatography (LC)-MS/MS detection was conducted using an ultra-performance liquid chromatography (UPLC) I-Class series Waters SYNAPT G2Si Quantitative Time-of-Flight mass spectrometer and a UPLC I-Class chromatographic system. Samples were precisely weighed, and 20-mg/mL solutions were prepared by adding 80 % methanol to each one. The samples were subsequently vortexed for 5 min and centrifuged at 13,000 rpm for 10 min before LC-MS/MS detection. A BEH C18 chromatographic column was used (100 mm × 2.1 mm, 1.8 μm), and the separation conditions were as follows: column temperature: 30 °C; and flow rate: 0.3 mL/min. The mobile phase contained 0.1 % formic acid (A) and acetonitrile (B), and the gradient elution procedure was as follows: 0–5 min, 80 % A; 5–23 min, 80%–0% A; and 23–25 min, 0–80 % A. The sample volume was 10 μL, and the detection wavelength was 254 nm. The following MS detection parameters were used: ion source: electrospray ionization; sample distribution detected in positive/negative electrospray ionization mode in the mass-to-charge ratio range of 50–1500; scanning mode: mode-scanning excitation; capillary voltage set to positive mode 2.5 kV/negative mode −2.5 kV; cone voltage: 20 V; source temperature: 150 °C; desolventizing temperature: 400 °C; flow rate of cone gas: 50 L/h; and flow rate of desolventizing gas: 500 L/h. The LockSpray was calibrated in real-time using leucine-enkephalin. MassLynx version 4.2 software (Waters, Shanghai) was used to extract and normalize the data detected in the positive and negative modes of the LC-MS/MS analysis.

2.5. Hematoxylin & eosin (HE) and Masson's trichrome staining

The tissue samples were fixed and preserved in 4 % formaldehyde solution, after which they were dehydrated and paraffin-embedded. The tissue was subsequently cut into 5-μm-thick transverse sections and subjected to HE and Masson's trichrome staining using standard techniques (Servicebio, G1003; Masson's staining solution, BASO, Zhuhai, BA4079). The staining was observed under a microscope (BX51, Olympus, Japan) for image capture or scanning. The HE staining was conducted to observe tissue structures and pathological changes before and after treatment. Masson's trichrome staining was conducted to visualize collagen fibers and cell nuclei in tissues, which appeared as blue and darker blue staining, respectively. ImageJ software was used to measure the area of collagen staining (blue) and the total tissue area, which were used to calculate the collagen volume fraction. The specimen slides were scored by a pathologist who was blinded to the study groups.

2.6. 16S rRNA sequencing

After euthanizing the mice with pentobarbital sodium, the colon contents were collected in sterile tubes, cryoprotected, and stored in a −80 °C freezer for follow-up testing. The fecal samples from the mice were analyzed by Majorbio Biotechnology Co., Ltd. (Shanghai, China). The extracted genomic DNA was subjected to 1 % agarose gel electrophoresis, and the barcoded universal bacterial primers 338F and 806R (5′-barcode-ACTCCTACGGGAGGCAGCA-3'/5′-GGACTACHVGGGTWTCTAAT-3′) were used to amplify the V3-V4 variable region of the 16S rRNA gene in triplicate. The resulting polymerase chain reaction products were further purified and quantified using an AxyPrep DNA Gel Extraction Kit (Axygen Biosciences, Union City, USA) and QuantiFluor-ST (Promega, Madison, USA). The purified amplicons were pooled in equimolar amounts and sequenced using a paired-end configuration on an Illumina MiSeq system (Illumina, San Diego, USA). Taxonomic analysis of OTU representative sequences at a 97 % similarity level was performed using the RDP classifier Bayesian algorithm, and the community species composition of each sample was statistically analyzed at each taxonomic level: Domain, Kingdom, Phylum, Class, Order, Family, Genus, and Species. The community diversity was reflected by using the Rank-abundance curve and Alpha diversity analysis. PCoA analysis was used to study the similarity or difference of sample community composition. Based on the community bar chart, analyze which dominant species each sample contains at a certain taxonomic level and the relative abundance (proportion) of each dominant species in the samples. The LEfSe analysis was used to identify the differential genera of microbiota. PICRUSt2 was used for functional prediction of the sequencing results. All further data analyses were evaluated using online tools from Majorbio (www.majorbio.com).

2.7. Immunohistochemical (IHC) staining

After deparaffinization, drops of endogenous peroxidase blockers were added to the tissue for a 10-min incubation at room temperature, after which the tissue was washed with double-distilled water. The slices were subsequently placed in ethylenediaminetetraacetic acid antigen retrieval solution, heated in a microwave at high temperature for 8 min, cooled to room temperature for 8 min, and re-heated in a microwave a second time at the same conditions. A 5 % bovine serum albumin blocking solution was added to the tissue for a 30-min incubation at 37 °C, after which the samples were incubated at 4 °C overnight in appropriately diluted primary antibody solutions. The primary antibodies included an anti-alpha smooth muscle actin (α-SMA) antibody (AF1032 Affinity), an anti-collagen I antibody (AF7001 Affinity), and an anti-transforming growth factor beta 1 (TGF-β1) antibody (AF1027 Affinity). The next day, the tissue was incubated at 37 °C for 30 min in a biotin-conjugated sheep anti-rabbit immunoglobulin G secondary antibody solution (SA1022 BOSTER), followed by 3,3′-diaminobenzidine staining. Finally, the samples were photographed under a microscope (BX51, Olympus, Japan) and scanned (APERIO VERSA 8, Leica). ImageJ software was

used to convert the image format and grayscale units into optical density units to quantify the area, density, and integrated optical density according to the manufacturer's protocol.

2.8. Enzyme-linked immunosorbent assay (ELISA)

Blood collected from the venous plexus of the medial canthus of the mice was centrifuged at 3000 rpm for 15 min, and the supernatant was collected for subsequent quantification of protein levels according to the ELISA kits' instructions. The following commercial kits were used in the present study: mouse adiponectin ELISA kit (MM-0547M2, MEIMIAN), mouse leptin ELISA kit (MM-0622M2, MEIMIAN), mouse TGF-β1 ELISA kit (MM-0135M2, MEIMIAN), and mouse connective tissue growth factor (CTGF) ELISA kit (MM-0077M2, MEIMIAN). The absorbance was measured at an excitation wavelength of 450 nm using a microplate reader (Synergy, BioTek, USA).

2.9. Statistical analysis

All data are presented as the mean ± standard deviation, with *t*-test analysis for comparisons between two groups and one-way ANOVA for multi-group comparisons. Statistical analyses were performed using GraphPad Prism 9.5.0 software (GraphPad Software, San Diego, USA). P values less than 0.05 were considered statistically significant.

3. Results

3.1. UPLC-MS/MS analysis of the main chemical components of SFZYD

The total ion flow diagram of SFZYD was obtained via UPLC-MS/MS analysis, and the data were processed using UNIFI software (Waters, Shanghai). A total of 157 SFZYD components were identified (Supplementary File), some of which included galloylpaeoniflorin, dehydrofumarin, quercetin, and kaempferol (Fig. 2A-B).

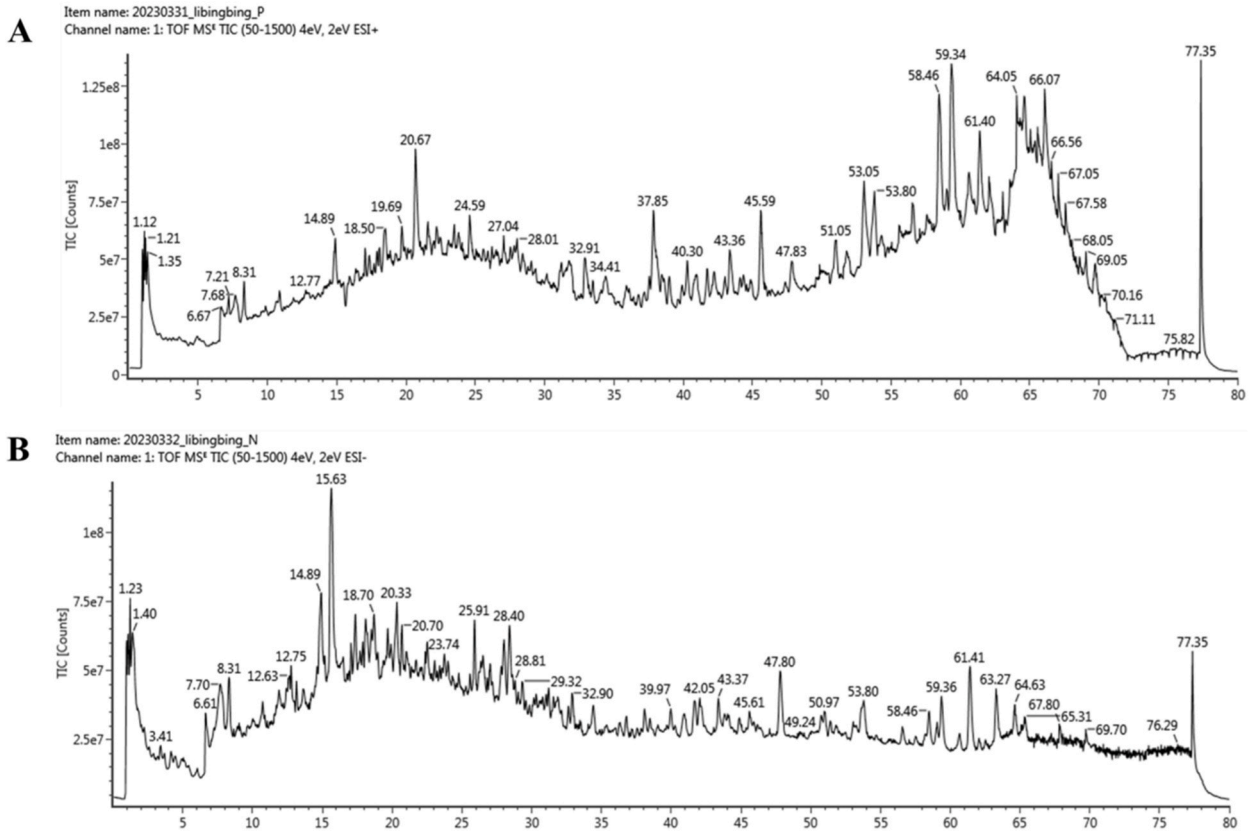

Fig. 2. The total ion flow diagram for SFZYD. (A) Positive ion mode; **(B)** Negative ion mode. SFZYD: Shaofu Zhuyu decoction; TIC, total ion chromatogram.

3.2. SFZYD treatment altered the cellular organization and reduced the weight of ectopic lesions

The body weights of the mice in the control, model, and SFZYD groups were measured on days 0, 7, 14, and 21 of the drug administration timeline; the results showed that the body weights of all three groups of mice decreased gradually over time (Fig. 3A). Gross observation revealed that the ectopic lesions were predominantly localized within the left abdominal wall of the mice. The cysts were either singular in number or grouped into multiple bead-like structures, with an irregular shape and a transparent or red–brown color. The surface and surrounding neovascularization of the cysts were visible, and adhesion with the surrounding tissues was occasionally evident. The release of cystic fluid was observed in cases in which rupture occurred during dissection, and the lesions exhibited evidence of angiogenesis on and around the surface. Following dissection, the ectopic cysts were revealed to be irregular in shape, polycystic in form, and transparent in appearance, with the longest diameter being approximately 15 mm (Fig. 3B). The weight of the ectopic tissue in the SFZYD group was significantly lower than that in the model group ($P < 0.05$) (Fig. 3C). The HE staining revealed that the uterine structure of the control group was clear and composed of the endometrial layer, myometrium, and outer membrane. The ectopic lesions of the mice in the model and SFZYD groups differed from the appearance of the normal uterus; for example, the tissue structure of the ectopic lesions was not transparent and could be distinguished based on the morphology of the histiocytes (Fig. 3D).

3.3. SFZYD treatment improved the intestinal microbial imbalance in mice with endometriosis

To obtain more robust evidence, 16S rRNA sequencing was conducted to assess the biological characteristics of the intestinal microbiota from the stool samples of mice in the control, model, and SFZYD groups (n = 6/group). A total of 10,629 operational taxonomic unit (out) sequences were collected; of them, only 2648 sequences were annotated as intestinal microbiota, including 1305 OTUs in the control group, 1822 OTUs in the model group, and 1268 OTUs in the SFZYD group (Fig. 4A). As shown in Fig. 4B, the curve gradually flattened out, indicating that the volume of sequencing data was sufficient, as verified by the rank abundance curves (Fig. 4B-C).

The Shannon and Simpson indices represent the diversity and richness of the intestinal microbiota, respectively. The statistical analysis of the alpha diversity revealed that compared to that of the control group, the model group exhibited a decreasing trend in alpha diversity, whereas compared to that of the model group, the SFZYD group exhibited an *increasing* trend, indicating that SFZYD treatment increased the abundance of the microbiota in mice with endometriosis (Fig. 4D). The beta diversity of the intestinal microbiota was evaluated based on the unweighted UniFrac-based principal coordinate analysis clustering results, which revealed separation between each of the groups and indicated that there were differences in the clustering results; these findings suggested a disorder of the intestinal microbiota in mice with endometriosis and that these changes could be affected by SFZYD treatment (Fig. 4E). Thus, modulation of the intestinal flora is one of the mechanisms through which SFZYD alleviates endometriosis.

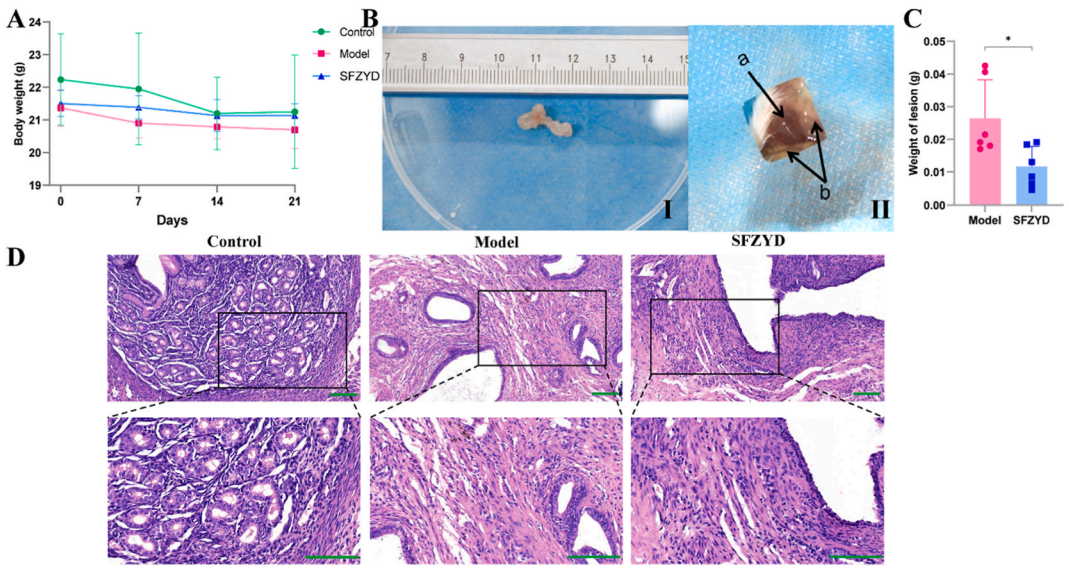

Fig. 3. Effect of SFZYD on body weight and lesion morphology in mice with endometriosis. (A) Body weight curve; **(B)** Representative images of ectopic lesions; **(C)** Lesion weights in the model and SFZYD groups; **(D)** Representative images of HE staining in each group. The scale bars represent 100 μm. Data are presented as the mean ± SD (n = 6). *$P < 0.05$ compared to the model group. SFZYD: Shaofu Zhuyu decoction; HE: hematoxylin & eosin.

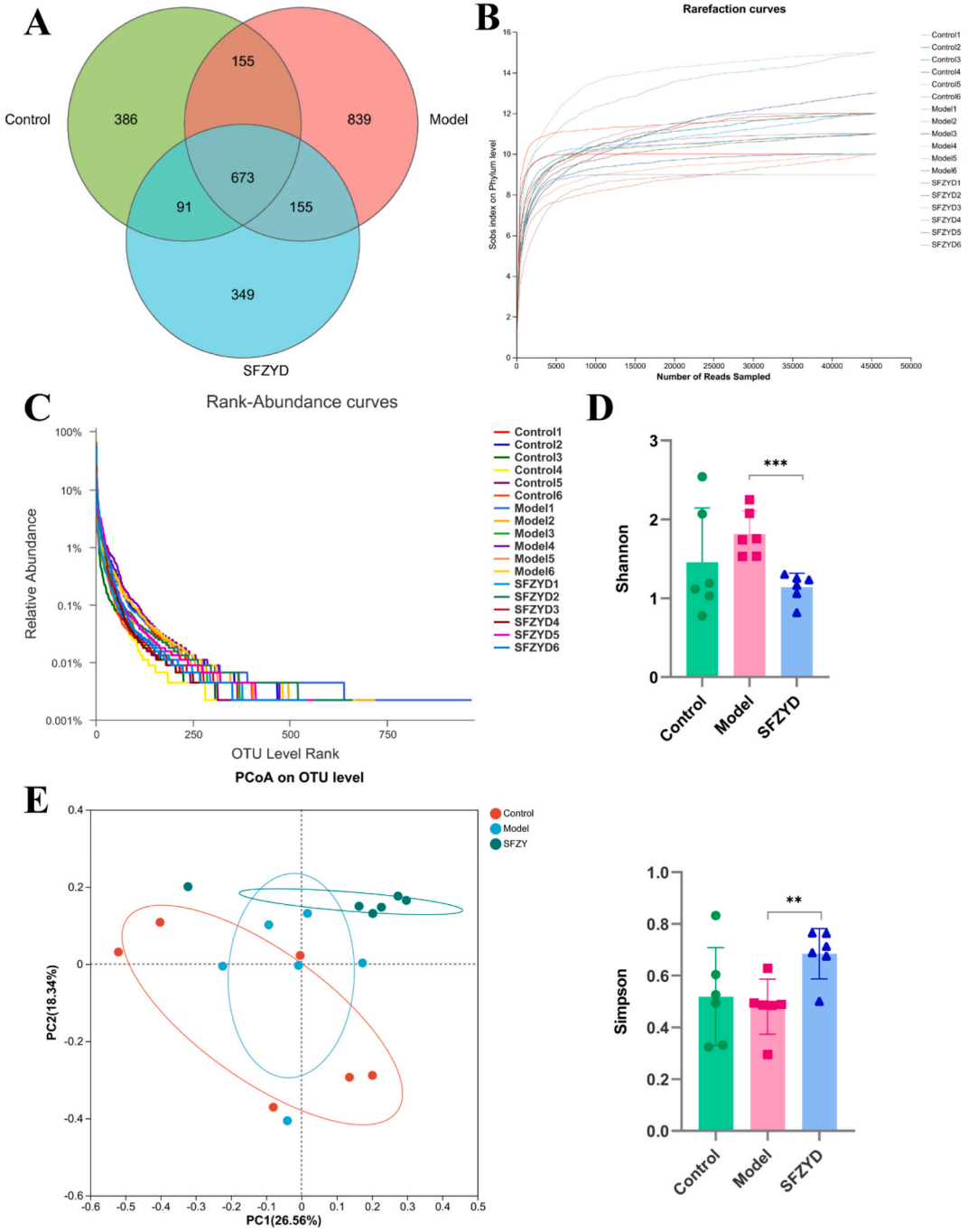

Fig. 4. SFZYD affects the abundance of intestinal microbes in mice with endometriosis. (A) Venn diagram of the number of OTUs in each group; **(B)** Rarefaction curve in each group; **(C)** Rank abundance curve in each group; **(D)** Shannon indices showing the α-diversity in each group; **(E)** PCoA plots on the OTU level in each group. Data are presented as the mean ± SD (n = 6/group). $^{***}P < 0.001$ and $^{**}P < 0.01$ compared to the model group. SFZYD: Shaofu Zhuyu decoction; Sobs, observed species; OTU: operational taxonomic unit; PCoA: principal coordinate analysis.

3.4. SFZYD treatment improved the intestinal microbiota of mice at the phylum, family, and genus levels

Differences in the taxonomic composition of the intestinal microbiota between the three groups were analyzed at the phylum, family, and genus levels. Bacteroidota, Firmicutes, and Verrucomicrobiota constituted a major proportion of all phyla in the three groups. In the control and model groups, the abundances of Bacteroidota, Firmicutes, and Verrucomicrobia were 34.67 % and 56.20 %, 56.29 % and 41.85 %, and 7.44 % and 0.10 %, respectively. The Firmicutes/Bacteroidetes ratio of the control group was 1.62, whereas

that of the model group was 0.74. The abundance of Bacteroidota in the SFZYD group was 82.70 % higher than that in the model group, whereas the abundance of Firmicutes in the SFZYD group was 16.29 %, which was lower than that in the model group. The abundance of Verrucomicrobiota in the SFZYD group was 0.03 %, which was also lower than that in the model group. This resulted in a lower Firmicutes/Bacteroidetes ratio in the SFZYD group (0.20) than in the model group (0.74) (Fig. 5A). At the family level, the top six microorganisms were Muribaculaceae, Lactobacillaceae, Lachnospiraceae, Bacteroidaceae, Akkermansiaceae, and Rikenellaceae (Fig. 5B). At the genus level, the top six microorganisms were norank_f_Muribaculaceae, Lactobacillus, Bacteroides, Akkermansia, Lachnospiraceae_NK4A136_group, and Alistipes (Fig. 5C).

Intergroup differences in intestinal microorganisms were further analyzed at the phylum, family, and genus levels. At the phylum level, there were significant differences in Bacteroidota ($P < 0.01$) between the three groups, and significant intergroup differences were observed at the family level for Muribaculaceae ($P < 0.01$) and Rikenellaceae ($P < 0.01$). Significant intergroup differences were observed at the genus level for norank_f_Muribaculaceae ($P < 0.01$) and unclassified_f_Ruminococcaceae ($P < 0.01$) (Fig. 5D–F).

Subsequent pairwise comparisons between the control and model groups and between the model and SFZYD groups revealed significant differences in Rikenellaceae ($P < 0.01$), Oscillospiraceae ($P < 0.05$), Tannerellaceae ($P < 0.05$) at the family level and in Alistipes ($P < 0.05$), norank_f_Oscillospiraceae ($P < 0.05$), and Rikenella ($P < 0.05$) at the genus level between the control and model groups, indicating that these microorganisms were closely related to the occurrence of endometriosis (Fig. 6A–B). There were also significant differences in Rikenellaceae ($P < 0.01$), Ruminococcaceae ($P < 0.01$), and Muribaculaceae ($P < 0.05$) at the family level, and in norank_f_Ruminococcaceae ($P < 0.01$), norank_f_Muribaculaceae ($P < 0.05$), and Desulfovibrio ($P < 0.05$) at the genus level

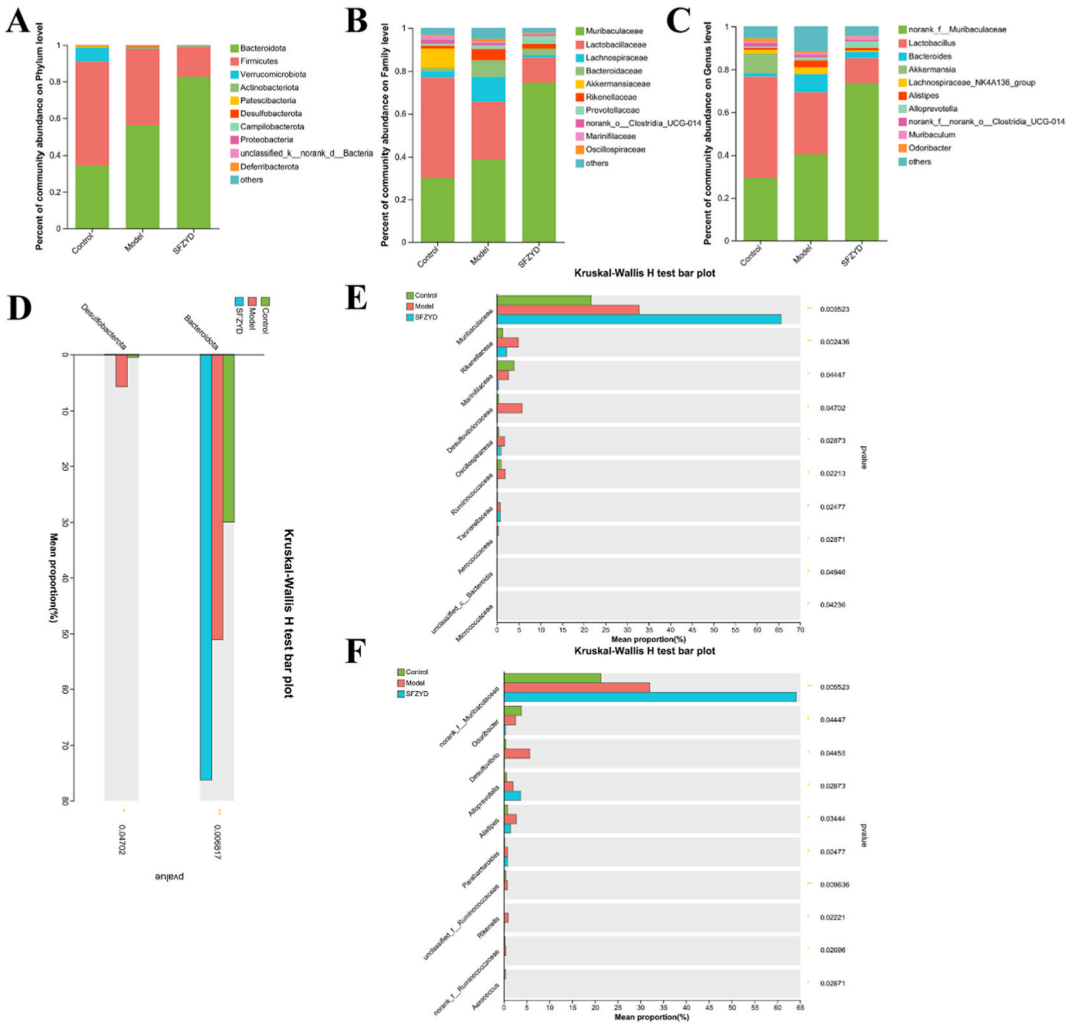

Fig. 5. SFZYD alters the composition of intestinal microbes in mice with endometriosis. (A) Bacterial abundance at the phylum level; **(B)** Bacterial abundance at the family level; **(C)** Bacterial abundance at the genus level; **(D)** Test for significance differences in bacterial composition between groups at the phylum level; **(E)** Test for significant differences in bacterial composition between groups at the family level; **(F)** Test for significant differences in bacterial composition at the genus level. Data are presented as the mean ± SD (n = 6/group). $^{**}P < 0.05$, $^{***}P < 0.01$. SFZYD: Shaofu Zhuyu decoction.

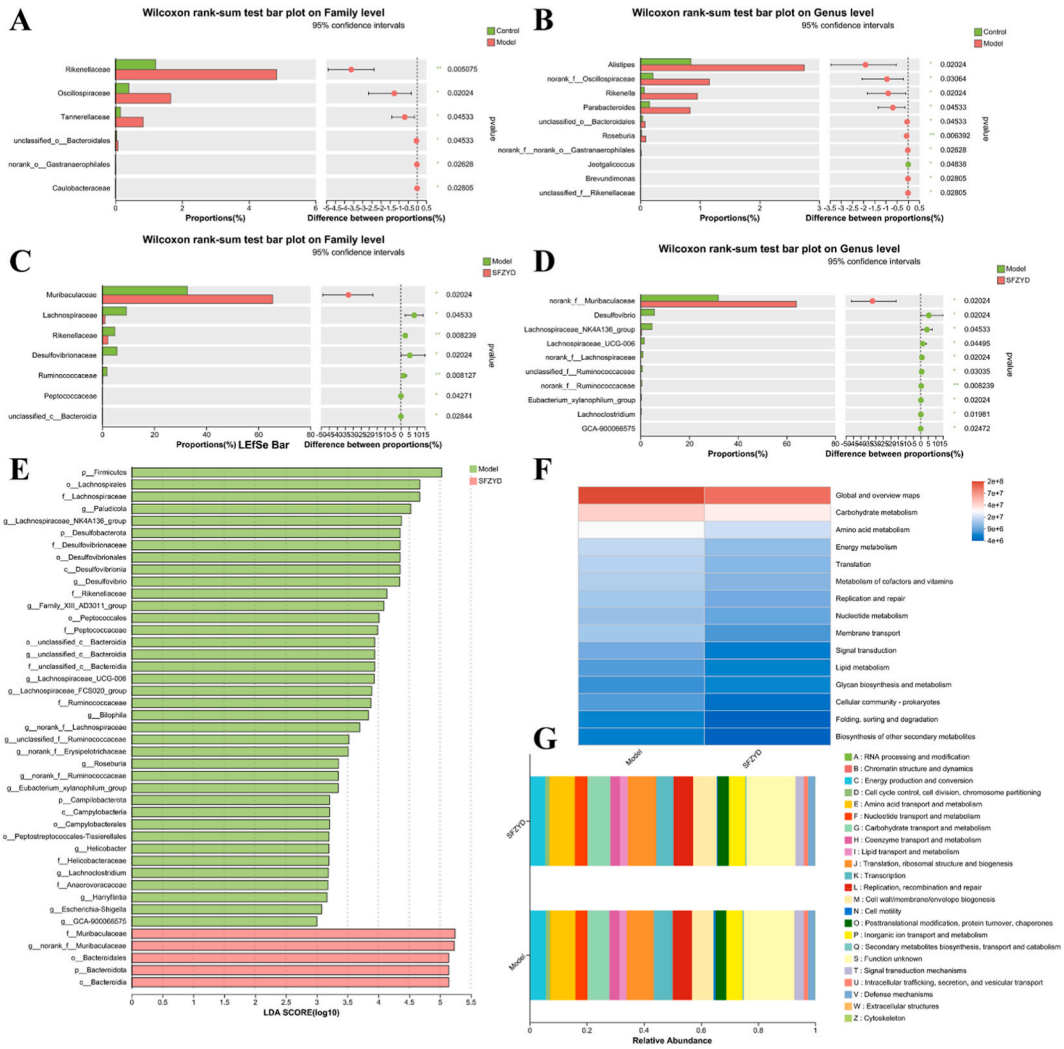

Fig. 6. Tests for significant differences between two groups and functional predictions. (A) Tests for significant differences between the Control and SFZYD groups at the family level; **(B)** Tests for significant differences between the Control and SFZYD groups at the genus level; **(C)** Tests for significant differences between the Model and SFZYD groups at the family level; **(D)** Tests for significant differences between the Model and SFZYD groups at the genus level; **(E)** LeFSe multi-stage discriminant analysis of species differences between the Model and SFZYD groups for the prediction of metabolic pathways using PICRUSt software; **(F)** KEGG functional abundance statistics; **(G)** GO functional abundance statistics. Data are presented as the mean ± SD (n = 6/group). $^{*}P < 0.05$, $^{**}P < 0.01$. SFZYD: Shaofu Zhuyu decoction; LDA: linear discriminant analysis: LeFSe, linear discriminant analysis effect size; PICRUSt: Phylogenetic Investigation of Communities by Reconstruction of Unobserved States 2; KEGG: Kyoto Encyclopedia of Genes and Genomes; GO: Gene Ontology.

between the control and model groups, suggesting that these microorganisms may play an important role in the mechanism through which SFZYT alleviates endometriosis (Fig. 6C–D). Furthermore, the linear discriminant analysis scores from the linear discriminant analysis effect size calculations revealed high expression levels of the microorganisms Desulfovibrio, Paludicola, Lachnospiraceae_NK4A136_group, Desulfovibrio, and Rikenellaceae in the intestines of mice with endometriosis, and treatment with SFZYD not only improved the symptoms of endometriosis but also enriched the levels of Muribaculaceae, norank_f_Muribaculaceae, Bacteroidales, and Bacteroidota (Fig. 6E).

3.5. SFZYD treatment improved endometriosis by regulating the composition of intestinal microbes in mice through the modulation of metabolic pathways

Kyoto Encyclopedia of Genes and Genomes (KEGG) and Gene Ontology (GO) functional abundance analyses were performed for the model and SFZYD groups using Phylogenetic Investigation of Communities by Reconstruction of Unobserved States 2 software. The analysis of the top 15 KEGG modules in terms of total abundance demonstrated that the differences in intestinal microbiota before and after SFZYD treatment were mainly related to carbohydrate, amino acid, and lipid metabolism pathways, among others (Fig. 6F). The

GO analysis showed that the biological functions of the intestinal microbiota in the model and SFZYD groups were similar and were predominantly related to amino acid transport and metabolism, translation, ribosomal structure, biogenesis, cell cycle control, cell division, and chromosome partitioning (Fig. 6G).

3.6. SFZYD treatment ameliorated endometriosis in mice through anti-fibrotic regulation

To further explore the mechanisms through which SFZYD alleviates endometriosis, its effects on energy metabolism were evaluated. Previous clinical studies have shown that patients with endometriosis commonly exhibit a lower body mass index and dysfunctional lipid metabolism, and the progression of the disease is closely related to the development of fibrosis. Masson's trichrome staining revealed that SFZYD treatment significantly reduced fibrosis in the ectopic lesions of mice ($P < 0.001$) (Fig. 7A). The results of

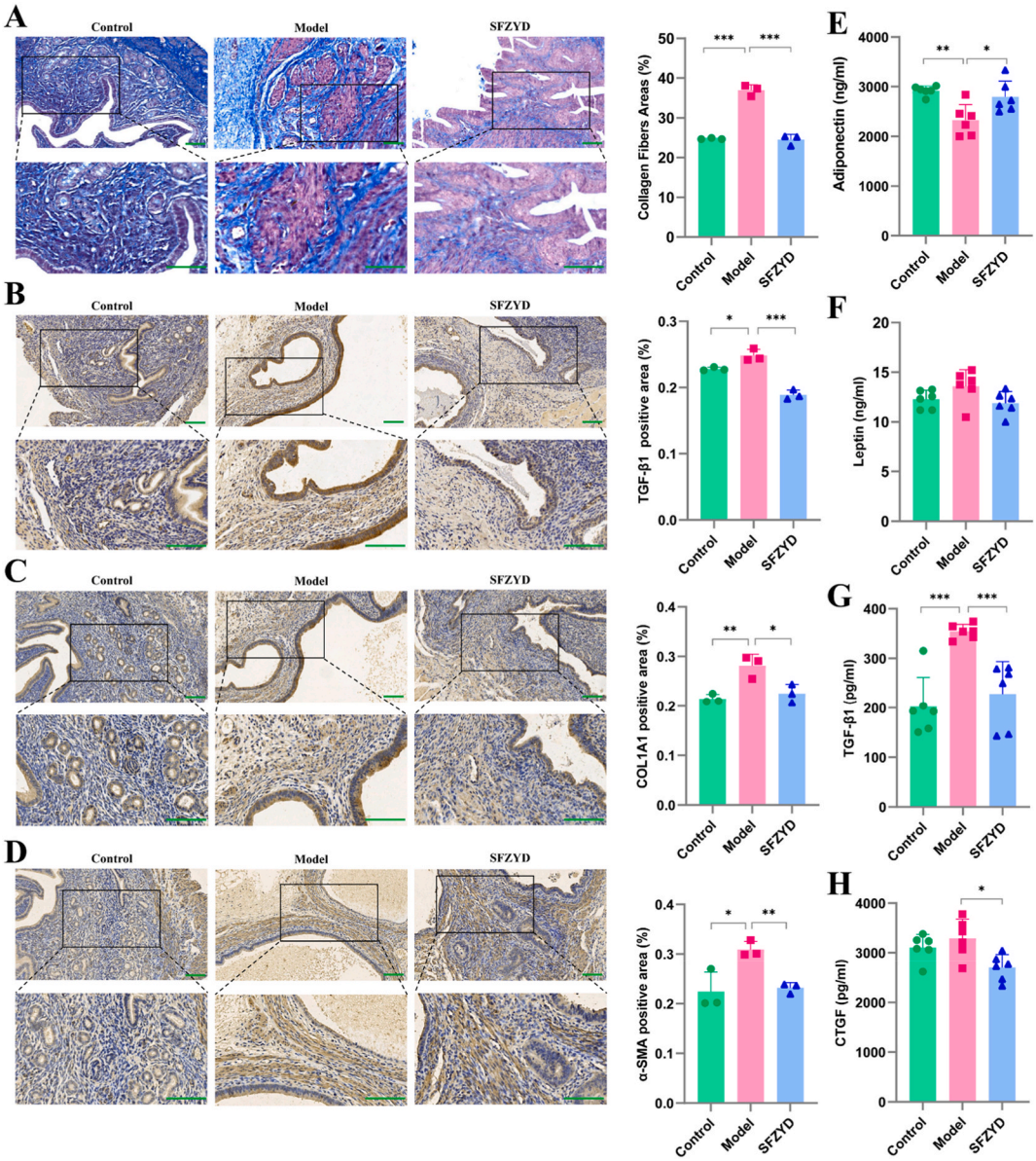

Fig. 7. SFZYD alleviates fibrosis in mice with endometriosis. (A) Representative images of Masson's trichrome staining and quantification of the proportion of collagen fiber area in each group; **(B–D)** representative images of IHC labelling and quantification of the expression of TGF-β1, COL1A1, and α-SMA, respectively, in each group; **(E–H)** Quantification of the protein expression levels of adiponectin, leptin, TGF-β1, and CTGF, respectively, in each group via ELISA. The scale bars represent 100 μm. Data are presented as the mean ± SD (n = 6/group). *$P < 0.05$, **$P < 0.01$, ***$P < 0.001$. SFZYD: Shaofu Zhuyu decoction; IHC: immunohistochemistry; TGF-β1: transforming growth factor beta 1; COL1A1: collagen type I alpha 1; α-SMA: alpha-smooth muscle actin; ELISA: enzyme-linked immunosorbent assay; CTGF: connective tissue growth factor.

the IHC labeling in ectopic lesions showed that the protein expression levels of TGF-β1 ($P < 0.001$) (Fig. 7B), collagen type I alpha 1 chain (COL1A1) ($P < 0.05$) (Fig. 7C), and α-SMA ($P < 0.01$) (Fig. 7D), all of which are related to fibrosis, were significantly decreased following SFZYD treatment. In addition, the ELISA results revealed that, compared to those in the model group, the serum levels of adiponectin were significantly higher ($P < 0.05$) (Fig. 7E) and serum levels of leptin were lower ($P > 0.05$) (Fig. 7F) in the SFZYD group; both of those proteins are related to lipid metabolism. SFZYD treatment also significantly reduced the expression levels of TGF-β1 ($P < 0.001$) (Fig. 7G) and CTGF ($P < 0.05$) (Fig. 7H), consistent with the IHC labeling results.

4. Discussion

Endometriosis is a disease in which endometriotic tissue forms at sites other than the uterus, and compounds used in traditional Chinese medicine such as SFZYD have played an important role in its treatment. SFZYD comprises 157 chemical components, including, but not limited to, galloylpaeoniflorin, dehydrofumarine, quercetin, and kaempferol. In the present study, the HE staining and lesionweight comparisons revealed that SFZYD treatment reduced the development of endometriotic lesions while delaying disease progression. Although the precise mechanisms of action are unknown, previous studies have explored the effects of SFZYD on a molecular level in the treatment of endometriosis, most of which have focused on inflammation, cell proliferation, angiogenesis, fibrosis, and invasion (Table 2), whereas the present study focused on changes in the gut microbiota and differences in energy metabolism.

The microbes in the gut comprise one of the most abundant microbiomes in the human body and are closely related to the absorption of nutrients and the establishment and maintenance of the immune system [25]. In addition to playing a role in the induction of various diseases of the gastrointestinal system, disturbances in the intestinal microflora can also affect the development or progression of many inflammatory and proliferative diseases via the modulation of immunity [26]. In recent years, scholars have proposed the existence of an "estrogen–gut microbiome axis," which closely links the composition or function of intestinal flora with various gynecological diseases [27]. For example, an experimental animal study demonstrated significant changes in the intestinal microbiomes of mice before and after intraperitoneal injection of endometrial tissue [28]. In another study, intestinal flora transplantation in mice with endometriosis promoted the development and progression of the disease; collectively, these findings suggested that the gut flora is a crucial regulator of endometriosis [29]. Huang et al. and Cao et al. reported that the alpha and beta diversity of the intestinal flora in groups with endometriosis were altered compared with those of the respective control groups in both human studies and animal experiments, which was basically consistent with the results of this study [30,31]. In the present study, compared with that of the control group, the model group exhibited a significantly increased abundance of *Rikenellaceae* ($P < 0.01$) at the family level and of *Alistipes* ($P < 0.05$) and *Rikenella* ($P < 0.05$) at the genus level. It is interesting to note that *Alistipes* and *Rikenella* are both members of the *Rikenellaceae* family and belong to the *Bacteroidota* phylum. Previous studies have shown that *Bacteroidota* could play a role in adiposity modulation through the production of short-chain fatty acids (SCFAs), acetate, and propionate [32]. Similarly, *Rikenellaceae* may contribute to a reduction in visceral fat mass [33]. At the family level, SFZYD treatment significantly reduced the abundance of *Lachnospiraceae* ($P < 0.05$), *Rikenellaceae* ($P < 0.01$), and *Ruminococcaceae* ($P < 0.01$), and at the phylum level, significant changes were observed for *Lachnoclostridium* ($P < 0.05$), *Lachnospiraceae_NK4A136_group* ($P < 0.05$), *LachnospiraceaE_NK4A136_group* ($P < 0.05$), *Lachnospiraceae_UCG-006* ($P < 0.05$), *norank_f_Lachnospiraceae* ($P < 0.05$), *unclassified_f_Ruminococcaceae* ($P < 0.05$), and *norank_f_Ruminococcaceae* ($P < 0.01$), which belong to *Lachnospiraceae* and *Ruminococcaceae,* respectively. Similar to *Rikenellaceae,*

Table 2
The mechanism of SFZYD in improving endometriosis.

Reference	Animal type	Molding method	Detection molecule	Phenotype
[12]	Sprague-Dawley rats	Autotransplantation	HIF-1α, microvessel density	Cell proliferation, cell apoptosis
[13]	BALB/c mice	Heterotopic transplantation	α-SMA, collange-I, PTEN、mTOR, Akt, p-Akt, p-mTOR	Fibrosis
[14]	SD rats	Autotransplantation	IL-6, IL-10, PGE2, TNF-α, MSK1, MSK2, DUSP1	Inflammation
[15]	SD rats	Heterotopic transplantation	TNF-α, IL-6, NK1, GPER2, MAPK, STAT1	Inflammation
[16]	SD rats	Autotransplantation	NOD1, RIP2, NF-κB, p65, IL-8, IL-18, TNF-α, COX-2	Inflammation
[17]	*Homo sapiens*	–	VEGF, MMP-9, IGF-1, NGF, SP, CGRP, BDNF, sFlt-1, PGE2, COX-2, TNF-α, IL-6	Inflammation, angiogenesis
[18]	*Homo sapiens*	–	RBP4, HMGB1, MCP-1, RANTES, PGE2、PGF2α、OT	Endometrial receptivity, inflammation
[19]	Wistar rats	Autotransplantation	5-HT, NO, PGF2α, Wnt, GSK-3β, TCF4, Frizzled, p-β-catenin, β-catenin	Invasion
[20]	SD rats	Autotransplantation	TNF-α, IL-6, IL-8, ERK, VEGF, MMP-9, NF-κB, MEK, MAPK	Inflammation
[21]	*Homo sapiens* primary cells	–	MMP-2, MMP-9	Invasion
[22]	*Homo sapiens* primary cells	–	Ang-1, Ang-2, Tie-2	Angiogenesis
[23]	SD rats	Autotransplantation	HIF-1α	–
[24]	–	–	IL6, PTGS2, VEGFA, FOS, IL-1B, ESR1	Inflammation, cell proliferation

Lachnospiraceae has the ability to hydrolyze starches and other sugars to produce butyrate and other SCFAs [34]. In addition, Shan et al. showed that *Blautia* and *Dorea*, which are members of *Lachnospiraceae*, were also highly expressed in patients with endometriosis and were associated with increased estradiol levels in the blood [35]. *Blautia* is a major producer of SCFAs, especially acetic acid, and reductions in *Blautia luti* and *Blautia* wexlerae are associated with insulin resistance in obese individuals. In addition, *Blautia* isolates prevent pathogen colonization by producing bacteriocins and exhibit anti-inflammatory properties and maintenance of glucose homeostasis by up-regulating the production of regulatory T cells and SCFAs. *Dorea* also has immunomodulatory effects, which may regulate the intestinal immune response and maintain the integrity and stability of the intestinal mucosal barrier by inducing Treg and inhibiting the differentiation and function of Th17 cells [36,37]. *Ruminococcus* has been identified as a potential intestinal biomarker for the diagnosis of endometriosis [38]. It is worth noting that *Ruminococcaceae* is one of the major bacterial producers of SCFAs. Lu et al. showed that SCFAs produced by *Ruminococcaceae* can reduce the expression of DNA methyl transferase 1, 3a, and 3b, as well as that of methyl-CpG binding domain protein 2; suppression of the binding of these enzymes can help correct the abnormal expression of adiponectin [39]. All of the top 15 pathways identified in the KEGG and GO analyses were found to be related to metabolic processes, indicating that endometriosis is closely associated with changes in metabolism.

There is increasing evidence suggesting that endometriosis is inversely associated with body mass index; however, the underlying mechanism remains unclear [40]. Dutta et al. and Zolbin et al. reported changes in fat metabolism in mice with endometriosis, and the BMI in these animals was affected by the presence of adipocytes as well as by fat metabolism [41,42]. Endometriosis is an estrogen-dependent disease, and adipocytes can affect disease progression by regulating estrogen secretion [43]. Adiponectin and leptin are both endogenously active adipocyte-secreted peptides that regulate energy in the body, with the levels of adiponectin and leptin being inversely proportional and directly proportional to the size of fat stores, respectively. Adiponectin is mainly involved in the regulation of energy homeostasis, especially lipid and glucose metabolism, as well as insulin sensitization, leading to improved insulin resistance [44]. Adiponectin contains a highly conserved complement factor C1q-like globular domain that binds to and activates its respective receptors, AdipoR1 and AdipoR2 [45], the former of which is predominantly expressed at high levels in skeletal muscle and the latter of which is highly expressed mainly in the liver. After binding to AdipoR1 and AdipiR2, adiponectin further exerts its effects mainly through the activation of adenosine monophosphate-activated protein kinase (AMPK) [46]. Processes downstream of AMPK mainly include those related to the inhibition of protein, lipid, and glycogen synthesis and fibrosis, the promotion of autophagy, and mitochondrial biogenesis [47]. Among the related factors, TGF-β is a key molecule involved in AMPK-mediated fibrosis, inducing the expression of CTGF in fibroblasts, thereby promoting myofibroblast differentiation and collagen synthesis [48]. The results of two meta-analyses of previous studies that investigated the roles of adiponectin and leptin showed that adiponectin was expressed at low levels, whereas leptin was highly expressed in patients with endometriosis [49,50]. Takemura and Choi et al. showed that AdipoR1 and AdipoR2 are expressed in the endometrium, and Takemura et al. demonstrated that adiponectin phosphorylates AMPK via AdipoR to maintain energy homeostasis and that it exerts anti-inflammatory effects during endometriosis [51,52].

A related feature of endometriosis is the presence of fibrotic tissue in and around the lesions, which can result in classic endometriosis-associated symptoms such as pain and infertility. The role of TGF-β in endometriosis-related fibrosis has been demonstrated, and CTGF is a key marker of fibrosis in fibrotic diseases, such as endometriosis and intrauterine adhesions [53]. In the present study, the Masson staining revealed that SFZYD treatment significantly reduced fibrosis in the ectopic tissues ($P < 0.001$), and the IHC labeling and ELISA results showed a significant overexpression of adiponectin ($P < 0.05$) in mice with endometriosis, along with higher levels of leptin ($P < 0.05$), TGF-β1 ($P < 0.001$), CTGF ($P < 0.05$), COL1A1 ($P < 0.05$), and α-SMA ($P < 0.01$); SFZYD treatment attenuated the changes in expression of all of these molecules.

There are still some shortcomings in this study: (1) The positive drug group was not set up during the experiment, and the efficacy of SFZYD in the treatment of endometriosis could not be objectively compared; (2) Although some key microbiota were identified in SFZYD treatment of endometriosis, whether SFZYD treatment of endometriosis is microbiota-dependent needs to be further verified by antibiotic inhibition experiments; (3) The anti-fibrosis effect of SFZYD on endometriosis requires further rescue experiments to verify; (4) in the process of SFZYD treatment of endometriosis, intestinal flora changes associated with the existence of the mechanism of anti-fibrosis still needs to be further defined.

In conclusion, the 16S rRNA analysis in the present study demonstrated that SFZYD treatment attenuated the changes in the intestinal microbiota caused by endometriosis, and the underlying mechanisms were mainly related to the regulation of carbohydrate, amino acid, and lipid metabolism. In addition, SFZYD treatment reduced the volume and fibrosis of ectopic lesions and improved metabolism, making it an effective treatment for endometriosis. Based on the intestinal flora and fiber into a breakthrough point, to explore the underlying mechanisms of SFZYD treatment of endometriosis, which will provide a scientific basis for research of traditional Chinese medicine treatment of endometriosis and new ideas, and provide guidance for SFZYD in clinical individualized application.

Ethical statement

All animal experiments were approved by the Animal Experiment Ethics Subcommittee of Jining Medical University (No. JNMC-2023-DW-150).

Funding

This study was supported by grants from the National Natural Science Foundation of China (No. 82104920), the Natural Science Foundation of Shandong Province (No. ZR2021QH129), the Shandong Provincial Key Laboratory of Traditional Chinese Medicine (No.

[2022]4), and the Shandong Medical and Health Science and Technology Development Plan Project (No. 202002040939).

Data availability statement

Data included in article/supp. material/referenced in article.

CRediT authorship contribution statement

Bing-Bing Li: Writing – review & editing, Methodology, Funding acquisition. **Qing-Qing Xun:** Methodology. **Chao Wei:** Methodology, Investigation, Formal analysis. **Bin Yu:** Visualization, Software, Methodology. **Xue Pan:** Writing – original draft, Visualization. **Qian Shen:** Writing – review & editing, Writing – original draft.

Declaration of competing interest

BBL designed and coordinated the study, performed the experiments, and acquired and analyzed the data; QQX and CW performed the experiments and acquired and analyzed the data; BY interpreted the data; and XP and QS wrote the manuscript. All authors have approved the final version of the article. The authors have no competing interests to declare that are relevant to the content of this article. All animal experiments were approved by the Animal Experiment Ethics Subcommittee of Jining Medical University (No. JNMC-2023-DW-150).

Acknowledgements

This study was supported by grants from the National Natural Science Foundation of China (No. 82104920), the Natural Science Foundation of Shandong Province (No. ZR2021QH129),the Shandong Provincial Key Laboratory of Traditional Chinese Medicine (No. [2022]4), and the Shandong Medical and Health Science and Technology Development Plan Project (No. 202002040939).

References

[1] P.T.K. Saunders, A.W. Horne, Endometriosis: etiology, pathobiology, and therapeutic prospects, Cell 184 (2021) 2807–2824, https://doi.org/10.1016/j.cell.2021.04.041.
[2] L. Saraswat, D. Ayansina, K.G. Cooper, S. Bhattacharya, A.W. Horne, S. Bhattacharya, Impact of endometriosis on risk of further gynaecological surgery and cancer: a national cohort study, BJOG 125 (2018) 64–72, https://doi.org/10.1111/1471-0528.14793.
[3] B. Ata, S. Yildiz, E. Turkgeldi, V.P. Brocal, E.C. Dinleyici, A. Moya, B. Urman, The endobiota study: comparison of vaginal, cervical and gut microbiota between women with stage 3/4 endometriosis and healthy controls, Sci. Rep. 9 (2019) 2204, https://doi.org/10.1038/s41598-019-39700-6.
[4] M.E. Salliss, L.V. Farland, N.D. Mahnert, M.M. Herbst-Kralovetz, The role of gut and genital microbiota and the estrobolome in endometriosis, infertility and chronic pelvic pain, Hum. Reprod. Update 28 (2021) 92–131, https://doi.org/10.1093/humupd/dmab035.
[5] S.B. Chadchan, S.K. Naik, P. Popli, C. Talwar, S. Putluri, C.R. Ambati, M.A. Lint, A.L. Kau, C.L. Stallings, R. Kommagani, Gut microbiota and microbiota-derived metabolites promotes endometriosis, Cell Death Discov 9 (2023) 28, https://doi.org/10.1038/s41420-023-01309-0.
[6] S.B. Chadchan, P. Popli, C.R. Ambati, E. Tycksen, S.J. Han, S.E. Bulun, N. Putluri, S.W. Biest, R. Kommagani, Gut microbiota-derived short-chain fatty acids protect against the progression of endometriosis, Life Sci. Alliance 4 (2021) e202101224, https://doi.org/10.26508/lsa.202101224.
[7] M. Leonardi, C. Hicks, F. El-Assaad, E. El-Omar, G. Condous, Endometriosis and the microbiome: a systematic review, BJOG 127 (2020) 239–249, https://doi.org/10.1111/1471-0528.15916.
[8] H. Itoh, T. Sashihara, A. Hosono, S. Kaminogawa, M. Uchida, Lactobacillus gasseri OLL2809 inhibits development of ectopic endometrial cell in peritoneal cavity via activation of NK cells in a murine endometriosis model, Cytotechnology 63 (2011) 205–210, https://doi.org/10.1007/s10616-011-9343-z.
[9] M. Bacci, A. Capobianco, A. Monno, L. Cottone, F. Di Puppo, B. Camisa, M. Mariani, C. Brignole, M. Ponzoni, S. Ferrari, P. Panina-Bordignon, A.A. Manfredi, P. Rovere-Querini, Macrophages are alternatively activated in patients with endometriosis and required for growth and vascularization of lesions in a mouse model of disease, Am. J. Pathol. 175 (2009) 547–556, https://doi.org/10.2353/ajpath.2009.081011.
[10] D. Ding, X. Liu, J. Duan, S.W. Guo, Platelets are an unindicted culprit in the development of endometriosis: clinical and experimental evidence, Hum. Reprod. 30 (2015) 812–832, https://doi.org/10.1093/humrep/dev025.
[11] S. Xu, R. Bian, X. Chen, Experimental Methodology of Pharmacology, third ed., People's Health Publishing House, Beijing, 2001 (China).
[12] G. Zhu, C. Jiang, X. Yan, S. Zhao, D. Xu, Y. Cao, Shaofu Zhuyu decoction regresses endometriotic lesions in a rat model, Evid Based Complement Alternat Med 2018 (2018) 3927096, https://doi.org/10.1155/2018/3927096.
[13] X.J. Ji, X.H. Zhang, C.C. Huang, Z.L. Zhang, H.Y. Mao, B. Yue, B.Y. Liu, Q.S. Wu, Shaofu Zhuyu decoction attenuates fibrosis in endometriosis through regulating PTEN/Akt/mTOR signaling pathway, Zhongguo Zhongyao Zazhi 48 (2023) 3207–3214, https://doi.org/10.19540/j.cnki.cjcmm.20221219.402. Chinese.
[14] Y.H. Chen, H.Y. Mao, Q.S. Wu, X.H. Zhang, J. Shen, P. Feng, C.C. Huang, X.J. Ji, Mechanism of Shaofu Zhuyu decoction in treatment of endometriosis-associated dysmenorrhea with syndrome of cold coagulation and blood stasis based on MSK1/2, Zhongguo Zhongyao Zazhi 47 (2022) 4674–4681, https://doi.org/10.19540/j.cnki.cjcmm.20220121.401. Chinese.
[15] Y.H. Cui, J. Wu, W. Cai, J. Du, J.M. Cao, X.J. Ji, Z.H. Gong, Molecular mechanism of Shaofu Zhuyu decoction in treating endometriosis dysmenorrhea based on GPER2/MAPK/STAT1 axis, Zhongguo Zhongyao Zazhi 43 (2018) 3362–3367, https://doi.org/10.19540/j.cnki.cjcmm.20180408.004. Chinese.
[16] H.Y. Mao, Y.H. Chen, X.J. Ji, Z. Wang, C.C. Huang, M. Li, X.H. Zhang, Q.S. Wu, Jiawei Shaofuzhuyu decoction inhibited the signal pathway to improve the ectopic endometrium and inflammatory microenvironment in rats with endometriosis dysmenorrhea, Lishizhen Medicine and Materia Medica Research 33 (2022) 2334–2338.
[17] H.Y. Mao, Y.H. Chen, Q.S. Wu, X.J. Ji, C.C. Huang, Y.M. Dou, X.H. Zhang, Effect of modified Shaofu Zhuyutang on neural angiogenesis and pelvic pain of endometriosis with syndrome of cold congeal and blood stasis, Chin. J. Exp. Tradit. Med. Formulae 28 (2022) 141–147, https://doi.org/10.13422/j.cnki.syfjx.20221295.
[18] T.F. Zhang, F. Mao, J.L. Zhao, Shaofuzhuyu decoction treating endometrial receptivity in patients with endometriosis and the influence of serum RBP4, HMGB1, MCP-1, RANTES, J. Chin. Med. Mater. 44 (2021) 210–214, https://doi.org/10.13863/j.issn1001-4454.2021.01.040.
[19] J.M. Cao, Discussion on Shaofu Zhuyu decoction based on Wnt/β-catenin signal pathway intervention study of model rats with endogenous dysmenorrhea[D], Gansu University of Chinese Medicine (2020), https://doi.org/10.27026/d.cnki.ggszc.2019.000137.
[20] J.X. Wang, Y.H. Cui, Y.X. Cheng, L.L. Fan, X.H. Zhang, D.Y. Fan, Effect of Shaofu-Zhuyu decoction on MAPK/ERK signaling pathway in rats with endometriosis, Chin. J. Pathophysiol. 35 (2019) 181–187.

[21] D.X. Yang, X.H. Wu, H.F. Cong, H.X. Kuang, Effect of drug serum containing Shaofuzhuyu Decoction on the secretion of MMP-2 and MMP-9 in endometriosis, Asia-Pacific Traditional Medicine 8 (2012) 3–4.
[22] D.X. Yang, H.X. Kuang, H.F. Cong, R. Zhao, Effect of drug serum containing shaofuzhuyu decoction on the secretion of Ang-1, Ang-2 and Tie-2 in endometriosis, Guide of China Medicine 10 (2012) 208–209, https://doi.org/10.15912/j.cnki.gocm.2012.06.015.
[23] Ying Cao, Sufen Bai, Du Chenguang, et al., Effect of Shaofuzhuyu decoction on HIF-1α expression in endometriosis model rats, Modern distance Education of Chinese Medicine 16 (2018) 94–96.
[24] Y.H. Chen, Z.L. Zhang, Q.S. Wu, P. Feng, X.Y. Qiao, X.H. Zhang, H.Y. Mao, S. Cai, X.J. Zhou, Mechanism of Shaofu Zhuyu decoction in treatment of EMT induced dysmenorrhea based on network pharmacology and molecular docking, Zhongguo Zhongyao Zazhi 46 (2021) 6484–6492, https://doi.org/10.19540/j.cnki.cjcmm.20210816.401.
[25] L.V. Hooper, D.R. Littman, A.J. Macpherson, Interactions between the microbiota and the immune system, Science 336 (2012) 1268–1273, https://doi.org/10.1126/science.1223490.
[26] J.M. Pickard, M.Y. Zeng, R. Caruso, G. Núñez, Gut microbiota: role in pathogen colonization, immune responses, and inflammatory disease, Immunol. Rev. 279 (2017) 70–89, https://doi.org/10.1111/imr.12567.
[27] J.M. Baker, L. Al-Nakkash, M.M. Herbst-Kralovetz, Estrogen-gut microbiome axis: physiological and clinical implications, Maturitas 103 (2017) 45–53, https://doi.org/10.1016/j.maturitas.2017.06.025.
[28] M. Yuan, D. Li, Z. Zhang, H. Sun, M. An, G. Wang, Endometriosis induces gut microbiota alterations in mice, Hum. Reprod. 33 (2018) 607–616, https://doi.org/10.1093/humrep/dex372.
[29] S.B. Chadchan, M. Cheng, L.A. Parnell, Y. Yin, A. Schriefer, I.U. Mysorekar, R. Kommagani, Antibiotic therapy with metronidazole reduces endometriosis disease progression in mice: a potential role for gut microbiota, Hum. Reprod. 34 (2019) 1106–1116, https://doi.org/10.1093/humrep/dez041.
[30] L. Huang, B. Liu, Z. Liu, W. Feng, M. Liu, Y. Wang, D. Peng, X. Fu, H. Zhu, Z. Cui, L. Xie, Y. Ma, Gut microbiota exceeds cervical microbiota for early diagnosis of endometriosis, Front. Cell. Infect. Microbiol. 11 (2021) 788836, https://doi.org/10.3389/fcimb.2021.788836.
[31] Y. Cao, C. Jiang, Y. Jia, D. Xu, Y. Yu, Letrozole and the traditional Chinese medicine, Shaofu Zhuyu decoction, reduce endometriotic disease progression in rats: a potential role for gut microbiota, Evid Based Complement Alternat Med 2020 (2020) 3687498, https://doi.org/10.1155/2020/3687498.
[32] Y. Lu, C. Fan, P. Li, Y. Lu, X. Chang, K. Qi, Short chain fatty acids prevent high-fat-diet-induced obesity in mice by regulating G protein-coupled receptors and gut microbiota, Sci. Rep. 6 (2016) 37589, https://doi.org/10.1038/srep37589.
[33] T. Tavella, S. Rampelli, G. Guidarelli, A. Bazzocchi, C. Gasperini, E. Pujos-Guillot, B. Comte, M. Barone, E. Biagi, M. Candela, C. Nicoletti, F. Kadi, et al., Elevated gut microbiome abundance of Christensenellaceae, Porphyromonadaceae and Rikenellaceae is associated with reduced visceral adipose tissue and healthier metabolic profile in Italian elderly, Gut Microb. 13 (2021) 1–19, https://doi.org/10.1080/19490976.2021.1880221.
[34] Y. Fan, O. Pedersen, Gut microbiota in human metabolic health and disease, Nat. Rev. Microbiol. 19 (1) (2021) 55–71, https://doi.org/10.1038/s41579-020-0433-9.
[35] J. Shan, Z. Ni, W. Cheng, L. Zhou, D. Zhai, S. Sun, C. Yu, Gut microbiota imbalance and its correlations with hormone and inflammatory factors in patients with stage 3/4 endometriosis, Arch. Gynecol. Obstet. 304 (2021) 1363–1373, https://doi.org/10.1007/s00404-021-06057-z.
[36] X. Liu, B. Mao, J. Gu, J. Wu, S. Cui, G. Wang, J. Zhao, H. Zhang, W. Chen, Blautia-a new functional genus with potential probiotic properties? Gut Microb. 13 (1) (2021) 1–21, https://doi.org/10.1080/19490976.2021.1875796.
[37] L. Fu, J. Song, C. Wang, S. Fu, Y. Wang, Bifidobacterium infantis potentially alleviates shrimp tropomyosin-induced allergy by tolerogenic dendritic cell-dependent induction of regulatory T cells and alterations in gut microbiota, Front. Immunol. 8 (2017) 1536, https://doi.org/10.3389/fimmu.2017.01536.
[38] R. Qin, G. Tian, J. Liu, L. Cao, The gut microbiota and endometriosis: from pathogenesis to diagnosis and treatment, Front. Cell. Infect. Microbiol. 12 (2022) 1069557, https://doi.org/10.3389/fcimb.2022.1069557. PMID: 36506023; PMCID: PMC9729346.
[39] Y. Lu, C. Fan, A. Liang, X. Fan, R. Wang, P. Li, K. Qi, Effects of SCFA on the DNA methylation pattern of adiponectin and resistin in high-fat-diet-induced obese male mice, Br. J. Nutr. 120 (2018) 385–392, https://doi.org/10.1017/S0007114518001526. Epub 2018 Jun 21. PMID: 29925443.
[40] A. Pantelis, N. Machairiotis, D.P. Lapatsanis, The Formidable yet unresolved interplay between endometriosis and obesity, Sci. World J. 2021 (2021) 6653677, https://doi.org/10.1155/2021/6653677.
[41] M. Dutta, M. Anitha, P.B. Smith, C.R. Chiaro, M. Maan, K. Chaudhury, A.D. Patterson, Metabolomics reveals altered lipid metabolism in a mouse model of endometriosis, J. Proteome Res. 15 (2016) 2626–2633, https://doi.org/10.1021/acs.jproteome.6b00197.
[42] M.M. Zolbin, R. Mamillapalli, S.E. Nematian, T.G. Goetz, H.S. Taylor, Adipocyte alterations in endometriosis: reduced numbers of stem cells and microRNA induced alterations in adipocyte metabolic gene expression, Reprod. Biol. Endocrinol. 17 (2019) 36, https://doi.org/10.1186/s12958-019-0480-0.
[43] J.I. Bjune, P.P. Strømland, R.Å. Jersin, G. Mellgren, S.N. Dankel, Metabolic and epigenetic regulation by estrogen in adipocytes, Front. Endocrinol. 13 (2022) 828780, https://doi.org/10.3389/fendo.2022.828780.
[44] H. Fang, R.L. Judd, Adiponectin regulation and function, Compr. Physiol. 8 (2018) 1031–1063, https://doi.org/10.1002/cphy.c170046.
[45] T. Yamauchi, J. Kamon, Y. Ito, A. Tsuchida, T. Yokomizo, S. Kita, T. Sugiyama, M. Miyagishi, K. Hara, M. Tsunoda, K. Murakami, T. Ohteki, et al., Cloning of adiponectin receptors that mediate antidiabetic metabolic effects, Nature 423 (2003) 762–769, https://doi.org/10.1038/nature01705. Erratum in: Nature 2004; 431:1123.
[46] H. Xu, Q. Zhao, N. Song, Z. Yan, R. Lin, S. Wu, L. Jiang, S. Hong, J. Xie, H. Zhou, R. Wang, X. Jiang, AdipoR1/AdipoR2 dual agonist recovers nonalcoholic steatohepatitis and related fibrosis via endoplasmic reticulum-mitochondria axis, Nat. Commun. 11 (2020) 5807, https://doi.org/10.1038/s41467-020-19668-y. Erratum in: Nat Commun 2021; 12:2036.
[47] J. Gao, J. Ye, Y. Ying, H. Lin, Z. Luo, Negative regulation of TGF-β by AMPK and implications in the treatment of associated disorders, Acta Biochim. Biophys. Sin. 50 (2018) 523–531, https://doi.org/10.1093/abbs/gmy028.
[48] J.G. Abreu, N.I. Ketpura, B. Reversade, E.M. De Robertis, Connective-tissue growth factor (CTGF) modulates cell signalling by BMP and TGF-beta, Nat. Cell Biol. 4 (2002) 599–604, https://doi.org/10.1038/ncb826.
[49] D.R. Kalaitzopoulos, I.G. Lempesis, N. Samartzis, G. Kolovos, I. Dedes, A. Daniilidis, K. Nirgianakis, B. Leeners, D.G. Goulis, E.P. Samartzis, Leptin concentrations in endometriosis: a systematic review and meta-analysis, J. Reprod. Immunol. 146 (2021) 103338, https://doi.org/10.1016/j.jri.2021.103338.
[50] Z. Zhao, Y. Wu, H. Zhang, X. Wang, X. Tian, Y. Wang, Z. Qiu, L. Zou, Z. Tang, M. Huang, Association of leptin and adiponectin levels with endometriosis: a systematic review and meta-analysis, Gynecol. Endocrinol. 37 (2021) 591–599, https://doi.org/10.1080/09513590.2021.1878139.
[51] Y. Takemura, Y. Osuga, T. Yamauchi, M. Kobayashi, M. Harada, T. Hirata, C. Morimoto, Y. Hirota, O. Yoshino, K. Koga, T. Yano, T. Kadowaki, et al., Expression of adiponectin receptors and its possible implication in the human endometrium, Endocrinology 147 (2006) 3203–3210, https://doi.org/10.1210/en.2005-1510.
[52] Y.S. Choi, H.K. Oh, J.H. Choi, Expression of adiponectin, leptin, and their receptors in ovarian endometrioma, Fertil. Steril. 100 (2013) 135–141, https://doi.org/10.1016/j.fertnstert.2013.03.019, e1-2.
[53] J.M. Garcia Garcia, V. Vannuzzi, C. Donati, C. Bernacchioni, P. Bruni, F. Petraglia, Endometriosis: cellular and molecular mechanisms leading to fibrosis, Reprod. Sci. 30 (2023) 1453–1461, https://doi.org/10.1007/s43032-022-01083-x.